JOURNAL OF MATERIALS SCIENCE **34** (1999) 6027–6033

Effect of micro-region heterogeneity on phase structure and dielectric properties in $Pb(Zn_{1/3}Nb_{2/3})O_3$-$PbTiO_3$-$BaTiO_3$ ceramics

XIAOLI WANG
School of Electronics and Information Engineering, Xi'an Jiaotong University, Xi'an, 710049, People's Republic of China
E-mail: xlwangl@xjtu.edu.cn

The phase structures of PZN-PT-BT ceramics under different synthesizing steps and thermal treatment were investigated. Although the calcinated powders (C.T. $= 900\,^{\circ}C$) of the compositions in tetragonal area exhibit pure tetragonal structure, the phase structures of the ceramics sintering at higher temperatures (S.T. $\geq 1080\,^{\circ}C$) are the mixtures of tetragonal and rhombohedral. The content of tetragonal phase in PZN-PT-BT ceramics decreases further after the specimens are annealed. Dielectric and ferroelectric properties were studied. The annealed ceramics have higher average phase transition temperatures, lower frequency dispersions, lower dissipation factors and larger aging rates. The maximum of the dielectric constant and the spontaneous polarization at room temperature are almost unaffected by annealing process. The concept of nano-phase separation is assumed to explain the experimental results. © *1999 Kluwer Academic Publishers*

1. Introduction

Micro-region heterogeneity is a common phenomenon both in compounds and in solid solutions with complex compositions [1–5]. That ferroelectrics of complex compounds and solid solutions exhibit broad phase transitions is generally taken to indicate the results of micro-compositional heterogeneity [6–9]. Expending the model of micro-region heterogeneity, nano-phase separation in solid solutions is anticipated to exist. The phenomenon of average phase transition temperature declining anomalously in $Pb(Zn_{1/3}Nb_{2/3})O_3$-$BaTiO_3$ (PZN-BT) ceramics with BT content increasing is illustrated using nano-phase separation [10, 11]. The Curie temperatures of $Pb(Zn_{1/3}Nb_{2/3})O_3$ and $BaTiO_3$ are 140 and 120 °C, respectively. But the average phase transition temperature of the solid solutions of PZN-BT system decreases sharply with the additive of BT. According to nano-phase separation model, para micro-regions of $Ba(Zn_{1/3}Nb_{2/3})O_3$ (BZN) are suggested to be present in PZN-BT ceramics. The anomalous decline of the average phase transition temperature in PZN-BT ceramics may be related to BZN para micro-regions.

$PbTiO_3$ is a ferroelectric with a high Curie temperature (490 °C) at which the phase transition from the cubic paraelectric phase (above Curie temperature) to the tetragonal ferroelectric phase (below Curie temperature). At room temperature, the structure of $PbTiO_3$ has the symmetry of the point group 4 mm with the ratio of axes $c/a = 1.063$, which is much larger than that of $BaTiO_3$ ($c/a = 1.01$). From the ferroelectric hysteresis loop of a $PbTiO_3$ single crystal, a spontaneous polarization of 52 μ c/cm^2 was determined [12]. When a solid solution is composed of $PbTiO_3$, and another perovskite ferroelectric other than tetragonal, there is always a morphotropic phase boundary (MPB) area in the solid solution system, such as $PbZrO_3$-$PbTiO_3$ (PZ-PT), $Pb(Mg_{1/3}Nb_{2/3})O_3$-$PbTiO_3$ (PMN-PT), $Pb(Zn_{1/3}Nb_{2/3})O_3$-$PbTiO_3$(PZN-PT) etc [13–15]. In traditional opinion, compositions in the area near MPB show diphase structures, whilst compositions far from MPB display single phase structure. In PZN-PT-BT ceramic system, a rhombohedral/tetragonal MPB was reported too (see Fig. 1) [16].

It has been found in my researches that the ceramics of PZN-PT-BT system located at the tetragonal area are not pure tetragonal structure, but the mixtures of rhombohedral and tetragonal phases. In this work, the phase structure of PZN-PT-BT ceramics under different synthesizing steps and thermal treatment were investigated. The variations of the structures and the dielectric properties were discussed using the model of nano-phase separation.

2. Experimental Procedure

In PZN-PT-BT system, the compositions selected for study were 0.80PZN-0.10PT-0.10BT, 0.75PZN-0.10PT-0.15BT, which are located at MPB area, and 0.75PZN-0.15PT-0.10BT, 0.70PZN-0.15PT-0.15BT, which are located at the tetragonal area. The columbite precursor method was used [17]. ZnO and Nb_2O_5 were batched in the proper ratio to first prepare the columbite phase $ZnNb_2O_6$ at 1000 °C for 6 h. The precursor was then wet mixed in stoichiometric ratio with PbO,

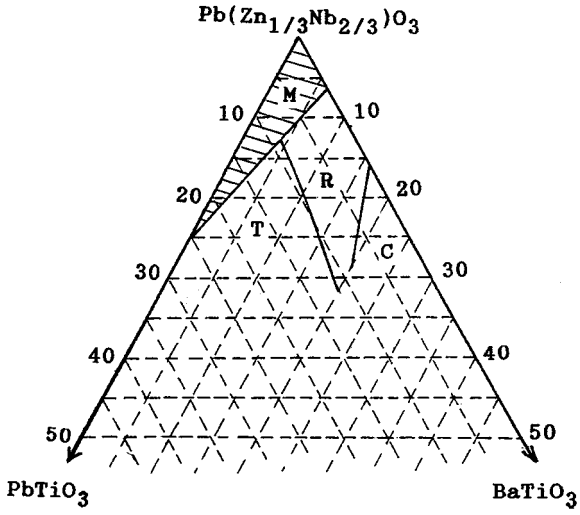

Figure 1 Phase diagram of $Pb(Zn_{1/3}Nb_{2/3})O_3$-$PbTiO_3$-$BaTiO_3$ system.

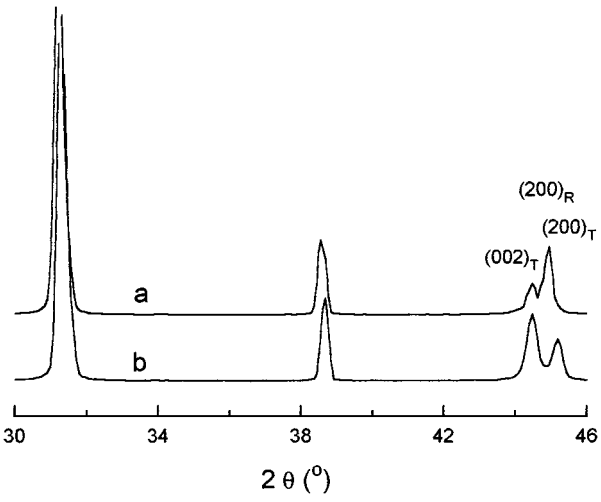

Figure 2 XRD patterns for 0.80PZN-0.10PT-0.10BT under different synthesizing steps, (a) calcinated (CT = 900 °C) powders, (b) ceramic sample (ST = 1100 °C). T: Tetragonal; R: rhombohedral.

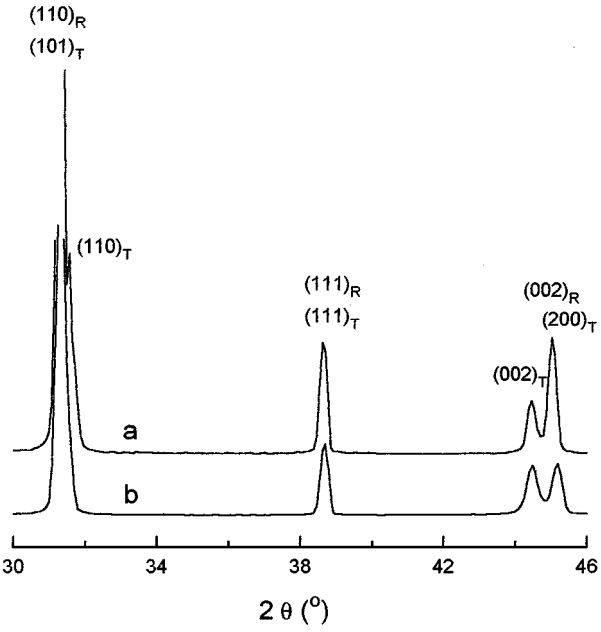

Figure 3 XRD patterns for 0.75PZN-0.15PT-0.10BT under different synthesizing steps, (a) calcinated (CT = 900 °C) powders, (b) ceramic sample (ST = 1100 °C).

$BaTiO_3$, and TiO_2. After drying, the mixtures were calcinated at 900 °C for 2 h in a sealed Al_2O_3 crucible. The powder X-ray diffraction (XRD) patterns indicate that all the compositions showed 100% perovskite phase. The calcinated powder was ball milled and dried again. Pellets 12 mm in diameter and 1–2 mm thick were pressed using 5% PVA binder. The binder was burnt out by slow heating up to 500 °C. Then the samples were sintered in a double-sealed Al_2O_3 crucible at temperature ranging from 1040 to 1140 °C for 1 to 2 h. To limited PbO evaporation from the pellets, a PbO-rich atmosphere was maintained by placing a equimolar mixture of PbO and ZrO_2 inside the crucible.

For electric measurements, the specimens were ground, electroded with silver paste, and fired at 550 °C for 10 min. Dielectric measurements were conducted on an automated system, wherein a temperature control box, a HP4274A (or a HP4275A) LCR meter were measured between 100 Hz and 400 kHz, as samples were heated at a rate of 3 °C/min. High field behavior was explored using a balanced Sawyer-Tower bridge under full program control.

After the electric measurements, the specimens were ground to remove silver electrode. The phase structures were detected for flat disks on a Rigaku D/MAX 2400 X-ray diffractometer with rotating anode using CuK_α radiation with a pyrolytic graphite monochromator. The scanning rate was 4°/min, with incremental step of 0.02°. Then, the specimens were annealed at 880 °C for 16 h in a double-sealed Al_2O_3 crucible under a PbO-rich atmosphere. All the measurements mentioned above were repeated on the specimens.

3. Experimental results

3.1. Structures

Figs 2 and 3 show the XRD patterns of 0.80PZN-0.10BT-0.10BT and 0.75PZN-0.15PT-0.10BT under different synthesizing steps, respectively. It is known that, from Fig. 1, both the compositions are in tetragonal area, only the former is in the vicinity of MPB. The XRD pattern profiles of plane family {2 0 0} are usually taken as evaluation of the coexistence of tetralgonal and rhombohedral phases for perovskites. For tetragonal phase, the diffraction intensity ratio of $I_{(200)}/I_{(002)}$ is about 2. Generally speaking, there should be three peaks around $2\theta = 45°$ in the XRD patterns of perovskite ceramics with coexistence of tetragonal/rhombohedral pahases, two peaks for tetragonal planes (0 0 2) and (2 0 0), and one peak for rhombohedral plane (2 0 0). In the vicinity of $2\theta = 45°$, however, only two sharp diffraction peaks were collected for both 0.80PZN-0.10PT-0.10BT and 0.75PZN-0.15PT-0.10BT. The structures of the two compositions look like pure tetragonal phase. Nevertheless, the fact is not so simple.

To facilitate discussion, the intensity of the two peaks around $2\theta = 45°$ are noted as I_{fro} and I_{bac}, respectively. The intensity ratio of I_{sec}/I_{fir} for the calcinated

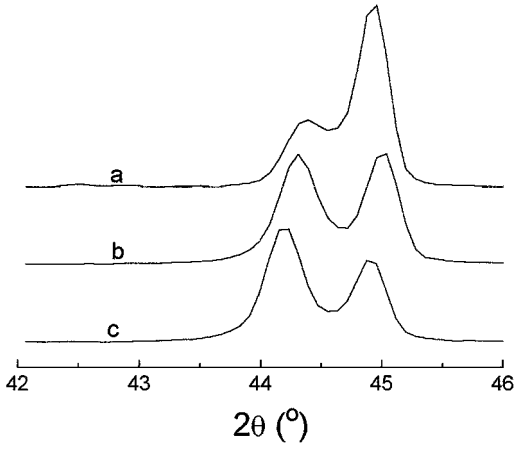

Figure 4 XRD patterns for annealed ceramic of 0.80PZN-0.10PT-0.10BT, (a) surface, (b) ground 33 μm away, and (c) ground 123 μm away.

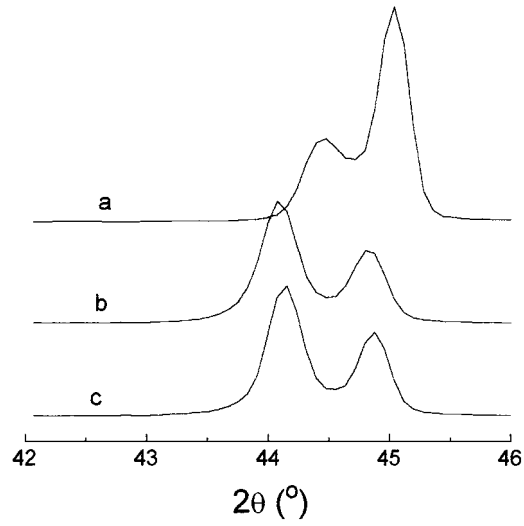

Figure 5 XRD patterns for annealed ceramic of 0.75PZN-0.15PT-0.10BT, (a) surface, (b) ground 40 μm away, and (c) ground 90 μm away.

powders of 0.80PZN-0.10PT-0.10BT and 0.75PZN-0.15PT-0.10BT are a little more than 2 (Fig. 2a and Fig. 3a). It seems that the tetragonal phase is the dominant part in the two compositions. However, after being sintered into ceramics at higher temperatures around 1100 °C, the XRD pattern profiles of both the compositions vary evidently in the same way. The intensity of the second reflection decreases and the first reflection increases (Fig. 2b and Fig. 3b). Table I lists the related XRD data.

To investigate the phase structure variation, the ceramic disks were annealed at 880 °C for 16 h in a double-sealed Al_2O_3 crucible under PbO-rich atmosphere. The XRD pattern of the same disk's surface of 0.80PZN-0.10PT-0.10BT ceramic is shown in Fig. 4a. The intensity of the front reflection decreases and the back reflection increases. The ratio of I_{bac}/I_{fro} larger than 3. In order to understand if there is any difference between the surface and the inside, the surface of the annealed ceramic disk was ground away about 33 μm in thickness. Fig. 4b is the XRD pattern of the ground face. Then another 90 μm were ground away further from the same disk side, and Fig. 4c is the XRD pattern of the second ground face. The XRD patterns of annealed 0.75PZN-0.15PT-0.10BT ceramic disk of the surface and the faces after grinding the surface off 40 and 50 μm more, respectively, are shown in Fig. 5. It can been seen from the results that there are structure differences between the surface and the inner for the annealed ceramic disks. Unlike that of the surface, the profiles of XRD patterns of the interior structure for the annealed ceramic disks are similar to those of the unannealed ones, and the ratio of I_{bac}/I_{fro} decline to some extent. Table II lists the XRD data. During XRD experiment, to eliminate the experiment errors, each sample was scanned three times on the same face, but on different area, that is, after one scanning, the ceramic disk was remounted again. The values of d and I are the arithmetic mean after three measurements. From Table II, the difference between d_{fro} and d_{bac} of interior is larger than that of surface for annealed samples.

Composition of 0.75PZT-0.10PT-0.15BT is located at rhombohedral region near MPB (Fig. 1). The XRD patterns of the ceramic disk on the same face, before and

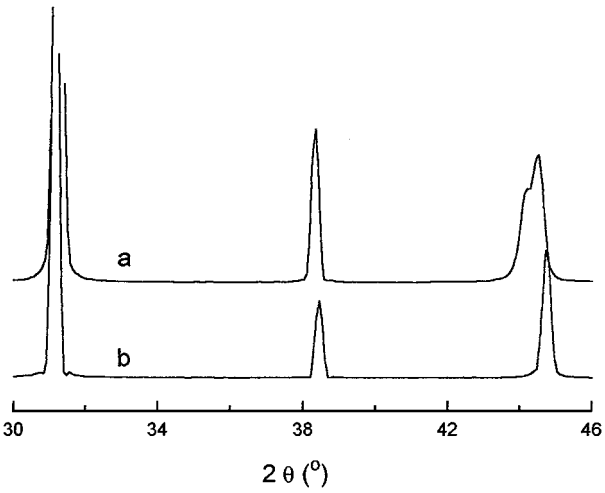

Figure 6 XRD patterns for unannealed (a) and annealed (b) ceramics of 0.75PZN-0.10PT-0.15BT.

after annealed, are shown in Fig. 6. Before annealed, the split of the reflection around 45° indicates that there is coexistence of rhombohedral/tetragonal phases in the sample. After annealed, however, only single reflection of (2 0 0) is left. It implicates only rhombohedral phase to have been detected through XRD.

Fig. 7 gives the XRD patterns on the same face of the ceramic disk 0.80PZN-0.05PT-0.15BT unannealed and annealed respectively. Comparing the diffraction peak profiles around 45°, the one before annealed is apparently not single diffraction peak, while the one after annealed is. It indicates that there exists a small amount of tetragonal phase in the ceramics that are located at rhombohedral area in Fig. 1. Annealing treatment eliminates the apparent tetragonal phase.

3.2. Dielectric properties

The dependents of dielectric constant and dissipation factor with temperature at different frequencies for the compositions of 0.80PZN-0.10PT-0.10, 0.75PZN-0.15PT-0.10BT, 0.70PZN-0.15PT-0.15BT, and 0.75

TABLE I XRD data for 0.80PZN-0.10PT-0.10BT and 0.75PZN-0.15BT-0.10BT

Composition	Calcinated at 800 °C				Sintered at 1100 °C			
	$\bar{d}_{fro}$ (nm)	$\bar{d}_{bac}$ (nm)	$\Delta\bar{d}$ (nm)	I_{bac}/I_{fro}	$\bar{d}_{fro}$ (nm)	$\bar{d}_{bac}$ (nm)	$\Delta\bar{d}$ (nm)	I_{bac}/I_{fro}
0.80PZN-0.10PT-0.10BT	0.2031	0.2014	0.0022	2.2	0.2036	0.2005	0.0031	0.63
0.75PZN-0.15BT-0.10BT	0.2038	0.2008	0.0030	2.1	0.2042	0.2012	0.0030	1.1

$\Delta\bar{d} = \bar{d}_{bac} - \bar{d}_{fro}$.

TABLE II Values of $\bar{d}$ in different depth of annealed ceramic disks for 0.80PZN-0.10PT-0.10BT and 0.75PZN-0.15PT-0.10BT

Composition	Measuring face	$\bar{d}_{fro}$ (nm)	$\bar{d}_{bac}$ (nm)	$\Delta\bar{d}$ (nm)	I_{bac}/I_{fro}
0.80PZN-0.10PT-0.10BT	Surface	0.2041	0.2016	0.0025	2.9
	Ground 33 μm away	0.2045	0.2015	0.0030	1.0
	Ground 123 μm away	0.2047	0.2015	0.0032	0.71
0.75PZN-0.15PT-0.10BT	Surface	0.2039	0.2013	0.0026	2.9
	Ground 40 μm away	0.2049	0.2017	0.0032	0.65
	Ground 90 μm away	0.2050	0.2018	0.0032	0.65

TABLE III Dielectric properties for compositions of 0.75PZN-0.15PT-0.10BT, 0.70PZN-0.15PT-0.15BT, and 0.75PZN-0.10PT-0.15BT

Composition	T_{max} (°C) (at 1 kHz)	ΔT_{max} (°C)	ε_{max} (at 1 kHz)	$\varepsilon_{20\,°C}$ (at 1 kHz)	$\tan\delta_{20\,°C}$ (at 1 kHz)
0.75PZN-0.15PT-0.10BT					
Unannealed	133	6	7600	2100	0.034
Annealed	167	0.17	7200	1900	0.0084
0.70PZN-0.15PT-0.15BT					
Unannealed	109	6	6900	2300	0.031
Annealed	160	0.31	6800	1900	0.010
0.75PZN-0.10PT-0.15BT					
Unannealed	80	12	7200	4700	0.043
Annealed	90	12	6500	4400	0.03

$\Delta T_{max} = T_{max,\,100\,kHz} - T_{max,\,100\,Hz}$.

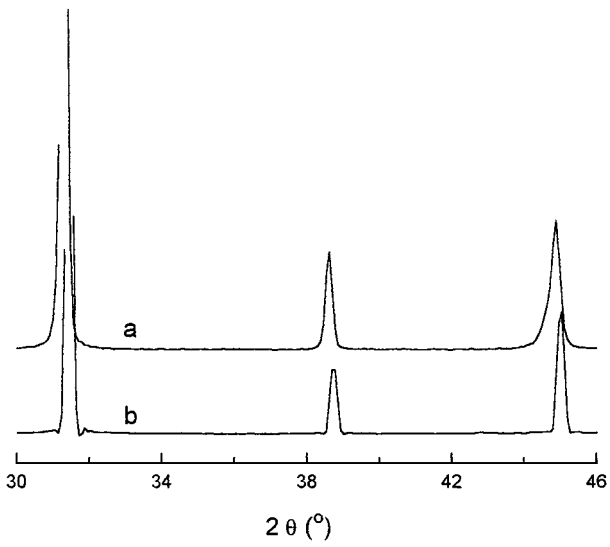

Figure 7 XRD patterns for unannealed (a) and annealed (b) ceramics of 0.80PZN-0.05PT-0.15BT.

PZN-0.10PT-0.15BT before and after annealed are shown in Fig. 8, respectively. Comparing with unannealed ones, the dielectric properties of the annealed samples for all four compositions vary similarly in some respects. For instances, the temperatures of the peak dielectric constants (T_{max}) shift towards higher temperatures, the frequency dispersion of dielectric constants and the dissipation factors before T_{max} declines. The dielectric data for the four compositions of 0.75PZN-0.15PT-0.10BT, 0.70PZN-0.15PT-0.15BT, and 0.75PZN-0.10PT-0.15BT are given in Table III.

Figs 9 and 10 show the ferroelectric hysteresis loops of 0.75PZN-0.10PT-0.15BT and 0.70PZN-0.15PT-0.15BT ceramics. The hysteresis loops of 0.75PZN-0.10PT-0.15BT are not affected by annealing from room temperature to 100 °C. For 0.70PZN-0.15PT-0.15BT, the hesteresis loops of the specimens both unannealed and annealed are identical around room temperature. With temperature increasing, the remanent polarization P_r of unannealed sample decreases sharplier than that of annealed one. When temperature is higher than 100 °C, though the values of P_r for unannealed and annealed specimen are same, the annealed ceramic has larger spontaneous polarization than unannealed one.

4. Discussions

In PZN-PT-BT system with BT content less than 10%, it is accepted that there is a MPB strip area in the vicinity of 10% of PT content (see Fig. 1). However, the results of XRD indicate that the ceramic phase structures of many PZN-PT-BT compositions in tetragonal phase area, even though PT content reaches 20%, are mixtures of tetragonal and rhombohedral phases.

Because of the micro-region heterogeneity, there could exist four sorts of micro-regions, PZN rich, PT rich, BT rich and BZN rich in PZN-PT-BT ceramics. The former three sorts of micro-regions are polar, while the last sort, BZN rich micro-region, is non-polar.

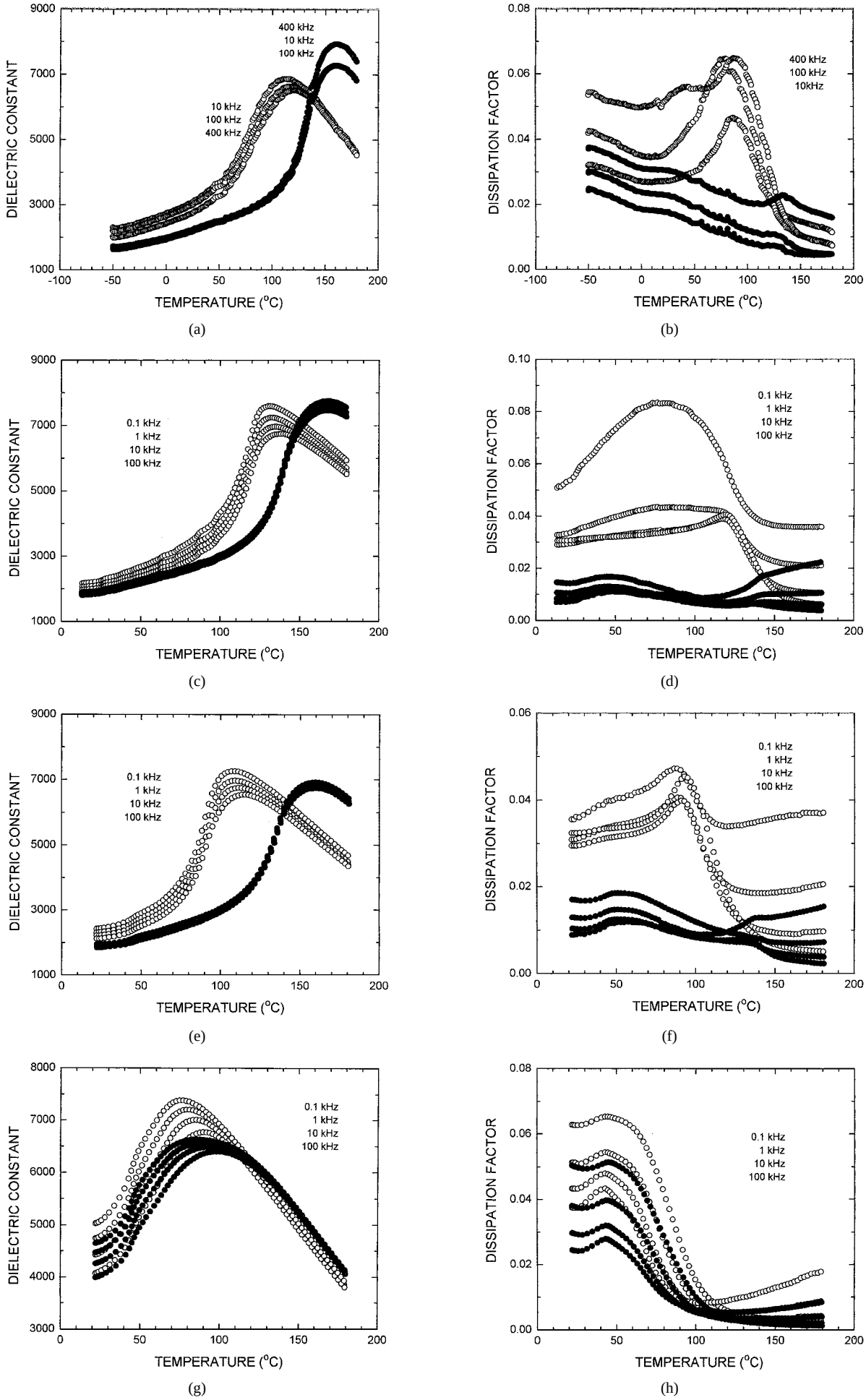

Figure 8 Temperature dependence of dielectric constant and dissipation factor at different frequencies for unannealed and annealed ceramics of 0.80PZN-0.10PT-0.10 (a) and (b), 0.75PZN-0.15PT-0.10BT (c) and (d), 0.70PZN-0.15PT-0.15BT (e) and (f), and 0.75PZN-0.10PT-0.15BT (g) and (h). Open circle: unannealed; Solid circle: annealed.

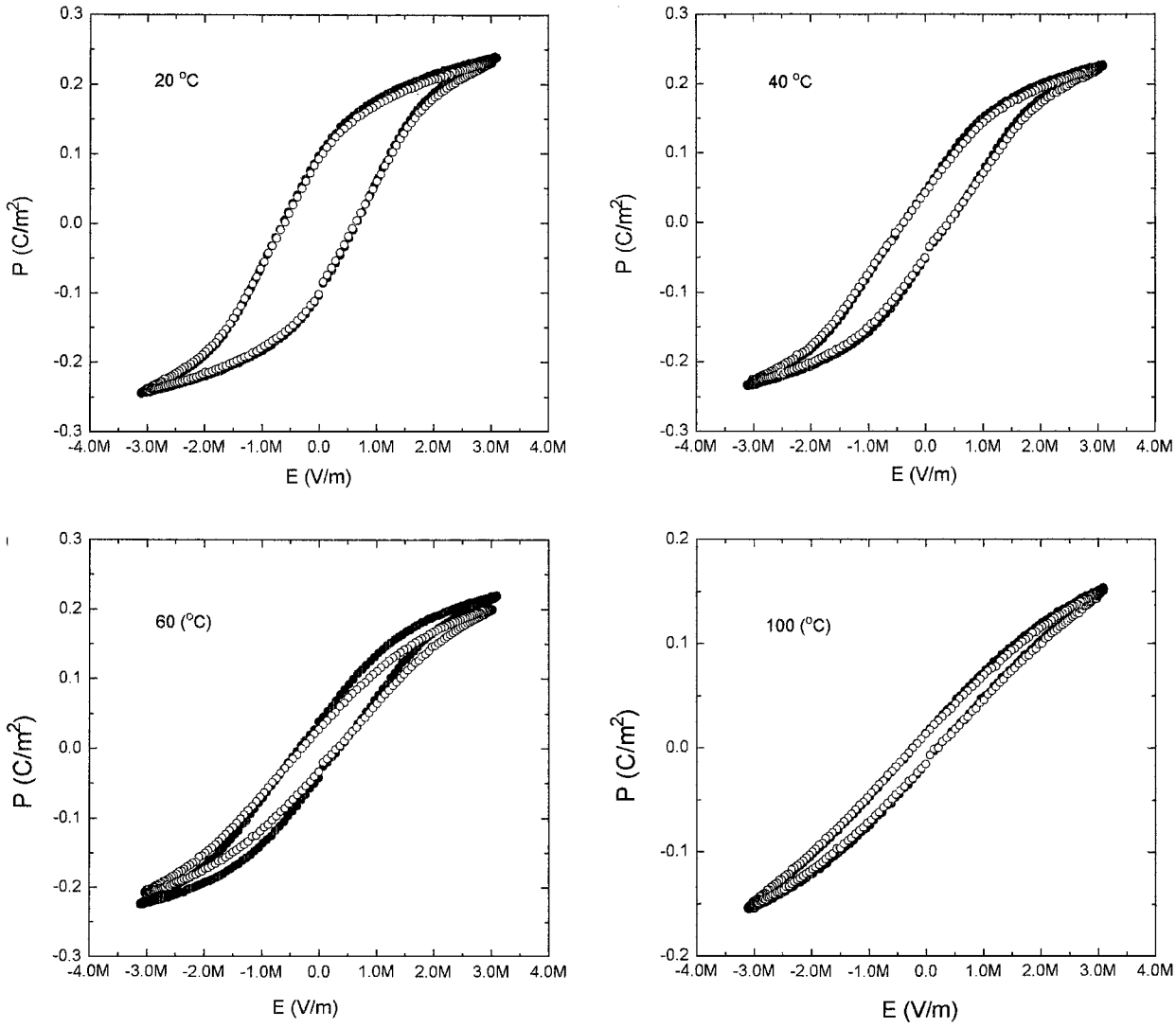

Figure 9 Ferroelectric hysteresis loops for unannealed and annealed ceramics of 0.75PZN-0.10PT-0.15BT at different temperatures. Open circle: unannealed; Solid circle: annealed.

The scales and amounts of these micro-regions are dependent on processing. The calcinated powders have more amount of inhomogeneous micro-compositions than the ceramic samples fired again at higher temperature. Through annealing, the inhomogeneity in the ceramic sample could lessen further. Therefore, both scales and amounts of PT rich micro-regions in the calcinated powders of PZN-PT-BT are larger and higher respectively than those of the ceramic samples are. If PT content is more than a certain extent in PZN-PT-BT system, the strong electric and elastic couplings among PT rich micro-regions could make the composition be pure tetragonal structure. Firing at higher temperature promotes various ions diffusing each other in the grains of ceramics, so that the scales and amounts of extreme inhomogenous micro-regions decrease, and the micro compositions are less inhomogeneous. The reduction of PT rich micro-regions weakens the static electric and elastic couplings among them, and tetragonal and rhombohederal phases coexist.

The experiments of PZN-PT-BT ceramics located at the tetragonal area in Fig. 1 coincide with the assumption above. The calcinated powders of 0.80PZN-0.10Pt-0.10BT, 0.75PZN0.15PT-0.10BT and 0.70 PZN-0.15PT-0.15BT show nearly single tetragonal structure, while their ceramic disks are diphases of tetragonal and rhombohedral. Annealing at 880 °C for 16 h deducts the amount of tetrahedral phase in the ceramic samples further. The percentage of tetragonal phase for 0.75PZN-0.10PT-0.15BT which located at the rhombohedral side near MPB of Fig. 1 decreases from less than 50% to about zero. The percentages of tetragonal phases for 0.75PZN-0.15PT-0.10BT and 0.70PZN-0.15PT-0.15BT which located at the tetragonal area of Fig. 1 lower from about 80% to about 60%.

Diffusion of ions in PZN-PT-BT ceramics during annealing process improves the micro-region heterogeneity and modifies their dielectric properties. The reduction of BZN rich non-polar micro-regions through annealing could make the average phase transition temperature increase [10]. As a matter of fact, annealed PZN-PT-BT ceramics exhibit higher average phase transition temperatures than unannealed ones. After annealing, the frequency dispersion of dielectric constant and the dissipation factors before T_{max} lessens distinctly, and the average phase transition temperatures (T_{max}) are independent of frequencies between 0.1 and 400 kHz. The results indicate that whether the perovskite ferroelectrics with complex compositions exhibit frequency dispersion does not depend on their

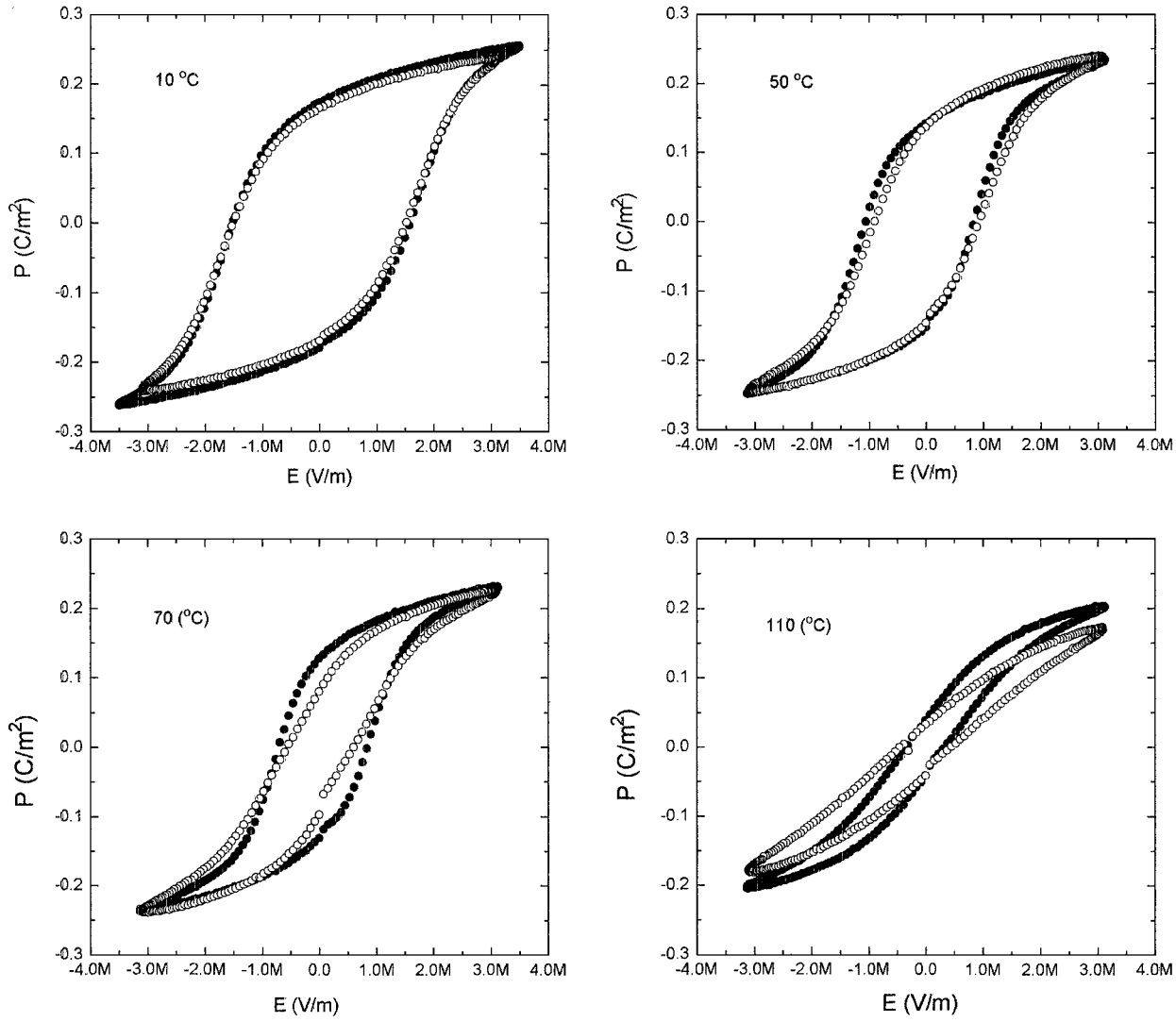

Figure 10 Ferroelectric hysteresis loops for unannealed and annealed ceramics of 0.70PZN-0.15PT-0.15BT at different temperatures. Open circle: unannealed; Solid circle: annealed.

phase structures, but on the conditions of their polar regions.

5. Summary

Many compositions in PZN-PT-BT ceramics synthesized using solid state reaction, besides the ones near the MPB, are mixtures of tetragonal/rhombohedral phases. The concept of nano-phase separation is introduced to understand the phenomenon. The scales and amount of PT rich polar micro-regions affect the apparent phase structure and the dielectric properties of a composition. In addition, there are BZN rich non-polar micro-regions in PZN-PT-BT ceramics, which could shift the average phase transition temperature.

Acknowledgements

The research was supported by the State Education Commission through the Trans-Century Training Program Foundation for the Talents.

References

1. B. KRAUSE, J. M. COWLEY and J. WHEATLEY, *Acta Cryst.* **A35** (1979) 1015.
2. C. A. RANDALL, D. J. BARBER, P. GROVE and R. W. WHATMORE, *J. Mater. Sci.* **23** (1988) 3676.
3. A. D. HILTON, C. A. RANDALL, D. J. BARBER and T. R. SHROUT, *Ferroelectrics* **93** (1989) 379.
4. M. P. HARMER, J. CHEN, P. PENG, H. M. CHAN and D. M. SMYTH, *ibid.* **97** (1989) 263.
5. D. VIEHLAND, N. KIM, Z. XU and D. A. PAYNE, *J. Amer. Ceram. Soc.* **78** (1995) 2481.
6. G. A. SMOLENSKII, Sov. *Jpn. J. Phys. Soc.* **28 (suppl.)** (1970) 26.
7. N. SETTER and L. E. CROSS, *J. Appl. Phys.* **51** (1980) 4356.
8. L. E. CROSS, *Ferroelectrics* **76** (1987) 241.
9. C. A. RANDALL and A. S. BHALLA, *IEEE 1990 Ultrasonic Symposium Proceedings* 711.
10. X. WANG and X. YAO, *Ferroelectrics* **145** (1993) 143.
11. *Idem., ibid.* **175** (1996) 165.
12. Y. XU, "Ferroelectric Materials and Their Applications" (North-Holland, 1991) p. 104.
13. K. KAKEGAWA, J. MOTRI, T. TAKAHASHI, H. YAMAMURA and S. SHIRASAKI, *Solid State Commun.* **24** (1977) 769.
14. S. W. CHOI, T. R. SHROUT, S. J. JANG and A. S. BHALLA, *Ferroelectrics* **100** (1990) 29.
15. S. NOMURA, M. YONEZAWA, K. DOI, N. TSUBOUCHI and M. TAKAHASHI, *NEC Res. Dev.* **29** (1973) 15.
16. A. HALLIYAL, U. KUMAR, R. E. NEWNHAM and L. E. CROSS, *J. Amer. Ceram. Soc.* **70** (1987) 119.
17. S. L. SWARTZ and T. R. SHROUT, *Mater. Res. Bull.* **17** (1982) 1245.

Received 18 November 1998
and accepted 20 April 1999